Soft Matter

PAPER

View Article Online
View Journal | View Issue

Cite this: *Soft Matter*, 2022, **18**, 2851

Evidence by neutron diffraction of molecular compounds in triarylamine tris-amide organogels and in their hybrid thermoreversible gels with PVC†

J.-M. Guenet, *[a] B. Demé,[b] O. Gavat,[a] E. Moulin[a] and N. Giuseppone[a]

Received 22nd February 2022,
Accepted 17th March 2022

DOI: 10.1039/d2sm00254j

rsc.li/soft-matter-journal

We report on neutron diffraction experiments performed on organogels prepared from triarylamine tris-amide (TATA), as well as on their ternary thermoreversible gels made up with poly[vinyl chloride] (PVC). Three different solvents together with their deuterated counterparts have been used; tetrachloroethane, wherein TATA fibrils display ohmic conductivity, bromobenzene and *o*-dichlorobenzene. The TATA crystal structure differs in the three solvents. Most importantly, the difference in the diffraction patterns whether hydrogenous solvents or deuterated solvents are used demonstrate the occurrence of molecular compounds. Tentative unit cells are presented. These results are also discussed in the light of the current views on the solvent role in the gelation process.

Introduction

Some specific properties of crystalline polymers are often determined by only one of the different crystalline lattices they can take on. A well-known example is provided by poly[vinylidene fluoride] that displays piezoelectricity only when under the so-called β form.[1,2] Another interesting case deals with clathrates of syndiotactic polystyrene/solvent that possess adsorbing properties of several pollutants thanks to the nanovoids obtained once the solvent has been extracted from the crystal lattice.[3,4] Conversely, the crystalline phase obtained from the bulk is not endowed with this property.

Recent investigations on triarylamine tris-amide (TATA) organogels have shown that their fibrillar gels display conductivity in certain solvents.[5,6] Although there are indications that the formation of radicals from the solvent molecule, namely 1,1,2,2-tetrachloroethane (TCE), is responsible for the phenomenon, little is known about the molecular structure, in particular the involvement of the solvent. The presence of the solvent in the crystalline lattice, resulting in the formation of molecular compounds,[7] has already been suggested for organogels,[8–11] and particularly for those prepared in this solvent as well as those obtained in ternary hybrid systems with poly[vinyl chloride] (PVC).[12,13]

Investigation of the role of the solvent in the molecular structure, particularly if molecular compounds are involved, implies to study the nascent state of the gels. Classical X-ray diffraction equipment that operate routinely at $\lambda = 0.154$ nm are not suited for studying TATA/TCE gels due to the high absorption coefficient of chlorine atoms ($\mu_{\text{X-ray}} \approx 107$ cm^2 g^{-1}). The use of a smaller X-ray wavelength, as available at synchrotron radiation facilities, provides photons of lower absorption coefficient ($\mu_{\text{X-ray}} \approx 15$ cm^2 g^{-1} for $\lambda = 0.08$ nm) yet not to the required extent. Similarly, drying the sample with the aim of overcoming the X-ray absorption issue is worthless as the molecular compound is to disappear under these conditions as will be shown in this paper.

To surmount these obstacles, we have performed neutron diffraction experiments, that are quite appropriate for tackling these issues thanks to the difference in scattering amplitude of hydrogenous solvents with respect to their deuterated counterpart.[14–17] This contrast property represents a decisive advantage of neutrons over X-rays since changing the solvent labelling allows one to differentiate readily a molecular compound from a solid phase.[15,16] In addition, the absorption coefficient of chlorine atom is about $\mu_{\text{N}} \approx 0.32$ cm^2 g^{-1} for neutrons,[18] namely up to 300 times lower than that of X-rays. Neutron diffraction therefore combines both the possibility of demonstrating the existence of compounds and of solving the X-ray absorption issue.

Here, we report on investigations carried out on TATA/solvent binary gels as well as TATA/PVC/solvent ternary gels prepared in three different solvents: 1,1,2,2-tetrachloroethane (TCE), bromobenzene (BrBz) and *o*-dichlorobenzene (*o*-DCB). We confirm the occurrence of molecular compounds in all three systems, yet with differing molecular packings of the TATA helices. Tentative unit cells are also presented.

[a] *Institut Charles Sadron, CNRS-Université de Strasbourg, 23 rue du Loess, BP84047, 67034 STRASBOURG, Cedex2, France. E-mail: jean-michel.guenet@ics-cnrs.unistra.fr*
[b] *Institut Laue-Langevin, 71 avenue des Martyrs CS 20156, 38042 GRENOBLE Cedex 9, France*

† Electronic supplementary information (ESI) available. See DOI: 10.1039/d2sm00254j

Experimental section

Materials

The fibrillar organogels were obtained from solutions of tri-aryl amines tris-amides designated as TATA-C11 in what follows (see Fig. 1). The synthesis and properties of these molecules are extensively described in ref. 5 and 6.

The poly[vinyl chloride], PVC, used for the preparation of the hybrid systems was purchased from Sigma-Aldrich and was used without further purification. The weight average molecular weight was found to be $M_w = 7.9 \times 10^4$ g mol^{-1} and the polydispersity index M_w/M_n = 1.87 by means of SEC in THF at 25 °C (universal calibration). The stereoregularity was determined by 13C-NMR. The fractions of tetrads were found to be sss = 41% ssi, iss, sis,... = 39% and iii = 19%.

ortho-Dichlorobenzene (*o*-DCBH), tetrachloroethane (TCEH) and bromobenzene (BrBzH) as well as their perdeuterated counterparts (*o*-DCBD, $C_6D_4Cl_2$), (TCED, $C_2D_2Cl_4$), (BrBzD, C_6D_5Br) were purchased from SigmaAldrich (purity grade 99.5%). All were used without further purification.

The preparation of the binary gels (PVC/*o*-DCB, TATA-C11/solvent) and of the hybrid networks (PVC/TATA-C11/solvent) consisted in heating appropriate mixtures up to 120–160 °C mixtures until clear, homogeneous solutions were obtained. Gels were produced by quenching these solutions at low temperature.

Two PVC concentrations have been studied: 4.82 × 10^{-2} g cm^{-3} (or 3.0 × 10^{-2} in g g^{-1}), designated as PVC5, 0.17 g cm^{-3} (or 0.11 in g g^{-1}) designated as PVC20. TATA concentration was varied from 3.8 × 10^{-2} g cm^{-3} (or 0.004 g g^{-1}) to 7 × 10^{-2} g cm^{-3} (or 0.065 g g^{-1}).

Neutron diffraction

Neutron diffraction experiments were carried out on the D16 camera located at Institut Laue-Langevin.[19] This instrument is equipped with a high-pressure helium detector of 320 × 320 mm^2 with 1 × 1 mm^2 pixels. The detector can rotate so as to access q values larger than those obtained on dedicated SANS instruments. In these experiments three angles were used: 0° for the transmission measurements, and 10.8° and 27° for determination of the diffracted intensities. The neutron wavelength is selected by beam reflection onto a focussing pyrolytic graphite monochromator. Experiments reported herein were obtained with a neutron wavelength of λ = 0.445 nm, providing the following q-range with the two-angle set-up: 0.6 nm^{-1} ≤ q ≤ 9 nm^{-1} (further details are available on https://www.ill.eu/users/instruments/instruments-list/d16/characteristics). The sample holder temperature was controlled with an external bath. Three temperature were used: T = 20 °C, T = 50 °C, and T = 70 °C. The raw data were further processed by subtracting the quartz cell, and correcting for the detector efficiency and solid angle by means of a vanadium sample (flat incoherent scattering). The neutron scattering amplitudes of the different components together with their X-ray counterparts are given in the Table S1 (ESI†).

The samples were prepared in closed quartz cells of 2 mm optical path purchased from B. Thuet (Blodelsheim, France). The required amounts of TATA and PVC powders are first introduced, and then mixed by stirring vigorously prior to addition of the solvent. The mixture is finally heated up to 160 °C. This procedure allows one to prepare more easily homogeneous solutions within a few minutes. Gels were formed by cooling the solutions in a fridge kept at 4 °C. Gel samples were systematically prepared in the same way whether hydrogenous or perdeuterated solvents were used.

Results and discussion

The general expression for the diffracted intensity by any kind of radiation for a binary system simply reads:

$$I(q) = \bar{A}_i^2(q)S_i(q) + \bar{A}_j^2(q)S_j(q) + 2\bar{A}_i(q)\bar{A}_j(q)S_{ij}(q) \qquad (1)$$

where, depending upon the subscript, $\bar{A}$ is the averaged scattering amplitude, and $S(q)$ the structure factor of the different

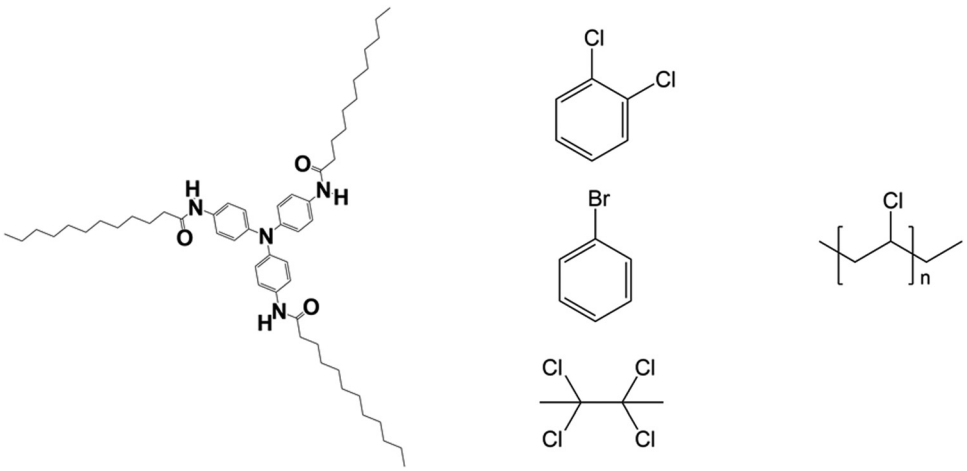

Fig. 1 Left: Chemical structure of the tri-aryl amine tris-amide C11 in its completely extended conformation. Center: *ortho*-Dichlorobenzene (*o*DCB), bromobenzene (BrBz), and tetrachloroethane (TCE); right PVC.

species, while $S_{ij}(q)$ is a cross-term related to the intermolecular terms between species.

In the present case, namely TATA fibrils and a liquid, there are two possible cases: (1) the solvent is totally excluded from the crystal unit cell, then $I(q)$ reduces to:

$$I(q) = \bar{A}_{\mathrm{TATA}}{}^2(q)S_{\mathrm{TATA}}(q) + \bar{A}_{\mathrm{solv}}{}^2(q)S_{\mathrm{solv}}(q) \qquad (2)$$

with obvious meaning for the subscripts.

Eqn (2) implies that changing the value of $\bar{A}_{\mathrm{solv}}$ will not alter the diffraction pattern of the crystalline TATA fibrils, in particular the relative intensity of the peaks with respect to one another as $S_{\mathrm{solv}}(q)$ is the structure factor of a liquid, chiefly featureless except for a broad maximum.

Conversely, if a molecular compound is formed, then the cross-term in relation 1 cannot be discarded any longer. Changing the contrast of the solvent, $\bar{A}_{\mathrm{solv}}$, is therefore to alter significantly the diffraction pattern.[15–17] The occurrence of molecular compounds can be demonstrated by comparing the diffraction patterns obtained by neutron diffraction of systems prepared in hydrogenous and in deuterated solvents as already shown for polymer–solvent molecular compounds.[15–17] Indeed, the scattering length of hydrogen ($a_{\mathrm{H}} = -0.375 \times 10^{-12}$ cm) differs drastically from that of deuterium ($a_{\mathrm{D}} = 0.670 \times 10^{-12}$ cm)[18] so that the neutronic contrast varies whether hydrogenous or deuterated molecules are considered (see Table S1, ESI†). This results in the variation of the peak intensity with the solvent labelling.[15–17] This rationale is also valid for ternary systems although eqn (1) contains additional terms.

(1) Binary systems TATA/solvent

Diffraction patterns obtained for TATA systems in hydrogenous solvents and deuterated solvents are shown in Fig. 2a–c. The diffraction patterns obtained by X-ray diffraction for the three existing structures in the solid state are provided for the sake of comparison (Fig. 2e).

There are two types of diffraction patterns depending upon the solvent type. TATA gels in bromobenzene and *o*-dichlorobenzene display virtually the same diffraction pattern, while that in tetrachloroethane differs significantly.

In all cases, the diffraction pattern for TATA/hydrogenous solvent differs from that in deuterated solvents. This effect is rather strong for systems in bromobenzene and in *o*-dichlorbenzene, but less pronounced with TCE. In the latter case, the relative intensities of the first 4 peaks depend upon the solvent labelling, which further confirms the occurrence of a molecular compound with this solvent (Fig. 2d).

The intensity of each reflection is calculated by integration of the peak after performing a fit with a Lorentzian function:

$$I(q) = S_{\mathrm{B}} + \frac{2C}{\pi}\left[\frac{\Delta q}{4(q-q_{\mathrm{o}})^2+\Delta q^2}\right] \qquad (3)$$

where q_{o} is the position of the peak, Δq is the full width at half maximum, S_{B} is the residual flat background and C is a calibration constant.

It is worth mentioning that the peaks 5 and 6 are absent in the TATA/TCEH systems unlike in their TATA/TCED counterpart (Fig. 2c), which is further consistent with the occurrence of a molecular compound.

The X-ray diffraction pattern previously reported on TATA/bromobenzene systems reveals only one peak[12] at q = 1.96 nm^{-1} (d = 3.2 nm) which also occurs here for TATA/bromobenzeneH. The use of deuterated bromobenzene instead reveals another two additional peaks at q = 3.469 nm^{-1} (d = 1.81 nm) and at q = 5.76 nm^{-1} (d = 1.091 nm) The positions of the peaks for TATA/*o*-DCB systems slightly differ with respect to those in bromobenzene (q = 2.005 nm^{-1}, d = 3.134 nm, q = 3.366 nm^{-1}, d = 1.867 nm, q = 5.483 nm^{-1}, d = 1.146 nm) although the diffraction pattern aspect is nearly the same. In the TATA/*o*-DCBH sample, very weak peaks are also seen at q = 3.366 nm^{-1} and q = 5.483 nm^{-1}. None of the structures observed in the TATA/*o*-DCB and TATA/bromobenzene gels correspond to the three structures observed in the solid state[13] (see Fig. 2e). This is not unexpected as the intercalation of solvent molecules is likely to alter the packing of the lateral TATA helices. In *o*-DCB and in Bromobenzene the first major peak is possibly related to the way TATA helices pack. It has been shown in a recent paper that one narrow peak only at q = 2.005 nm^{-1} can be theoretically reproduced for TATA/bromobenzene gels when one considers TATA helices packed in straight rows without intermolecular correlation instead of a hexagonal packing.[13]

The equation used for calculating the diffracted intensity is that of hollow cylinders, which pertains to helical structures at low resolution:[20,21]

$$I(q) \sim \frac{\pi\mu_{\mathrm{L}}}{q}\left[\frac{2A_{\mathrm{in}}}{A_{\mathrm{m}}qr_{\mathrm{out}}}J_1 q\gamma r_{\mathrm{out}} + \frac{2A_{\mathrm{out}}}{A_{\mathrm{m}}qr_{\mathrm{out}}} \times \{J_1(qr_{\mathrm{out}}) - \gamma J_1(q\gamma r_{\mathrm{out}})\}\right]^2 \times \sum_{j=1}^{n}\sum_{k=1}^{n} J_{\mathrm{o}}(qd_{jk}) \qquad (4)$$

where A_{in}, A_{out} and r_{in} the radius of the inner cylinder, and r_{out} are the scattering amplitudes and the radii of the inner cylinder and of the outer hollow cylinder, respectively, with $\gamma = r_{\mathrm{in}}/r_{\mathrm{out}}$, and $A_{\mathrm{m}} = \gamma^2 A_{\mathrm{in}} + [1-\gamma^2]A_{\mathrm{out}}$, with $A_{\mathrm{in}}/A_{\mathrm{out}} = 4.03$, d_{jk} the distance between the axis of cylinders j and k, n the number of cylinders, and J_1 and J_{o} Bessel functions of first type and order 1 and order 0, respectively.

In eqn (4) the first term corresponds to the cylinder inscribing the helix, and the second term depends on the helix packing. As is shown in Fig. S1 (ESI†), arranging helices in rows unlike in a hexagonal packing allows one to reproduce the FWHM.

On these considerations a possible model is portrayed in Fig. 2 (compound **1**) where TATA helices display correlation within rows, while adjacent rows are not correlated. In addition, the handedness of helices is randomly distributed.[13]

Alternatively, the appearance of new peaks for TATA/BromobenzeneD and TATA/*o*-DCBD possibly correspond to the arrangement of the solvent molecules within the compound (q and corresponding d values are summarized in Table S2, ESI†). Attempting to place the solvent molecules would be too

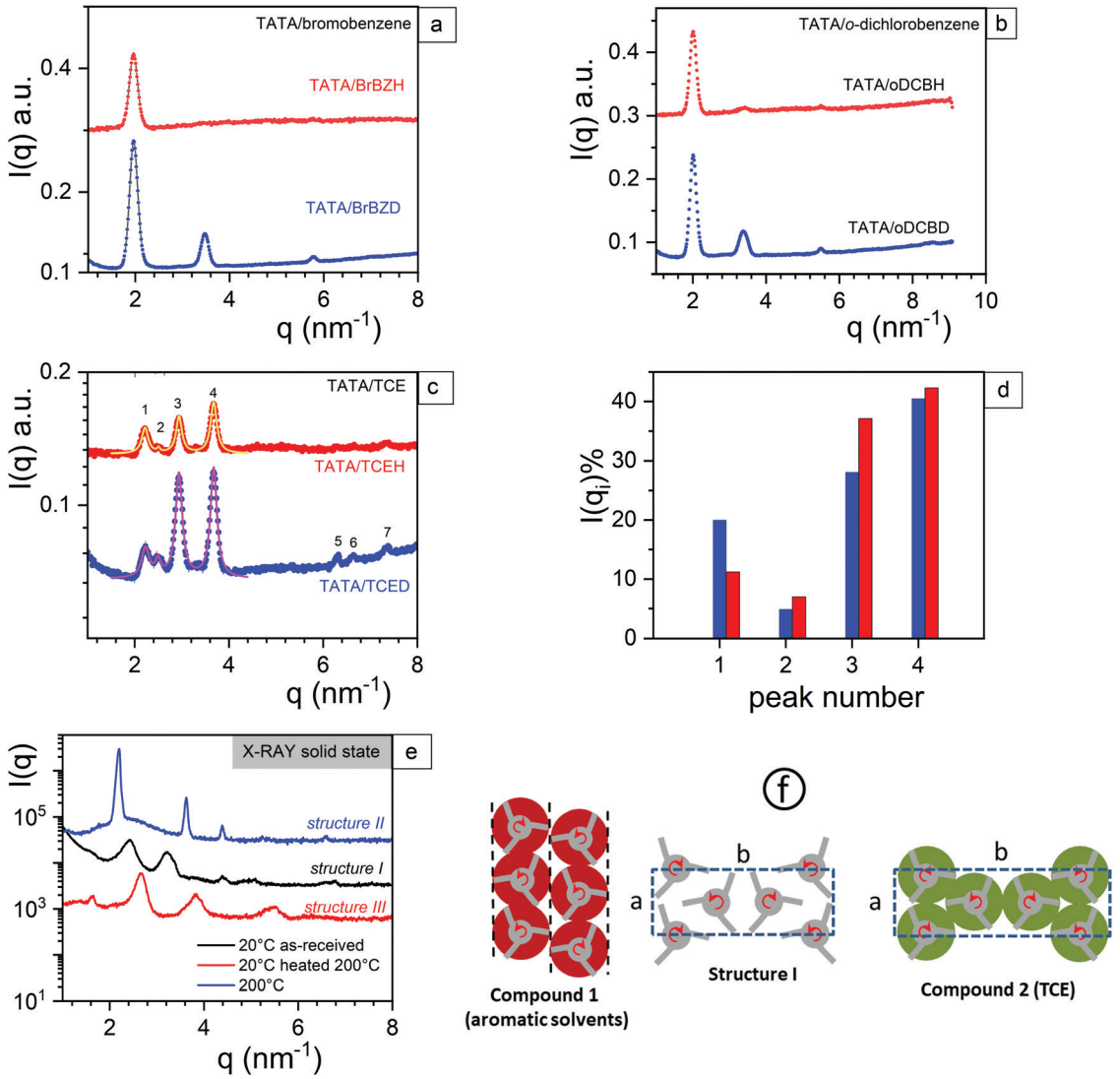

Fig. 2 (a) Neutron diffraction pattern for TATA/bromobenzene (C_{TATA} = 0.07 g cm^{-3}); (b) neutron diffraction pattern for TATA/*o*-dichlorobenzene (C_{TATA} = 0.07 g cm^{-3}); (c) neutron diffraction pattern for TATA/tetrachlorethane (C_{TATA} = 0.07 g cm^{-3}). The full lines correspond to a fit with Lorentzian functions (relation 3); (d) relative intensities of the first five peaks *vs.* the solvent labelling as determined by the fit with Lorentzian functions (relation 3), blue = TCED, red = TCEH (e) X-ray diffraction pattern for TATA in the solid state from ref. 13. (f): helix packing in structure **I** from ref. 13, and tentative for compounds, see text. For compound **1** (left), red, hollow discs are used for representing the solvation shell with bromobenzene; correlation between TATA helices occurs only within the rows highlighted by dashed lines. Rows are not correlated, right and left-handed helices are randomly distributed. For compound **2** (right) a tentative orthorhombic unit cell reminiscent of that of solid I except that the TATA helices are wrapped in a solvent shell (green, hollow discs). For details about the lattice parameters see ESI.†

much speculative with the data at hand. These peaks related to the solvent may correspond to *hk*0 plane but also to 00*l* planes. One may therefore contemplate the possible insertion of these aromatic solvents between the phenyl groups of the TATA molecules, which would entail the occurrence of another helical structure differing from the 20_1 previously reported.[5,6] Determination of the helical structure by diffraction experiments requires oriented samples to find out whether these peaks correspond to equatorial or to meridional reflections. Orienting these gels is, however, quite difficult as they are easily breakable. DFT calculation may possibly throw some light on this issue.

In the case of TATA/TCE gels there is no drastic modification of the diffraction pattern whether hydrogenous or deuterated TCE are used except modifications of the relative peak intensity (Fig. 2d). A part is probably due to the small difference in the scattering amplitude of TCEH and TCED (see Table S1, ESI†), but may also suggest a lower the degree of helix solvation with respect to bromobenzene and *o*-dichlorobenzene.

A tentative orthorhombic unit cell as portrayed in Fig. 2f (compound **2**) has been derived from these data by considering one of the previous published structures observed in the solid state (structure I, see Fig. 2e).[13] As previously discussed,[13] only the 2D packing of the helices is considered as there is no

special correlation along the 3rd dimension (*c*-axis), hence, only *hk* Miller indices are given. Basically, it is surmised that this structure is a solvated version of structure **I**. The visible seven peaks can be accounted for by considering a monoclinic unit cell with a = 2.98 nm, b = 10.04 nm and $\gamma = 90^\circ$. The a and b parameters are larger than those of structure **I**, which indeed points to a swollen version of this structure **I** arising from helix solvation. Details and peak assignation are summarized in Table S3 (ESI†), and the agreement with the experimental and calculated values is shown in Fig. S2 (ESI†).

These results again show that the molecular structure depends upon the solvent type, as is expected for molecular compounds. These outcomes further provide another example where the Hansen solubility parameter, although qualitatively indicative, is not necessarily relevant for predicting the gelation behaviour of this organic molecule.[11,22–24] Tetrachloroethane and Bromobenzene possess very close solubility parameters (19.8 and 20.3, respectively[25]), and yet their gelation behaviour in these solvents is totally distinct both from the thermodynamic aspect, as melting points and formation temperatures

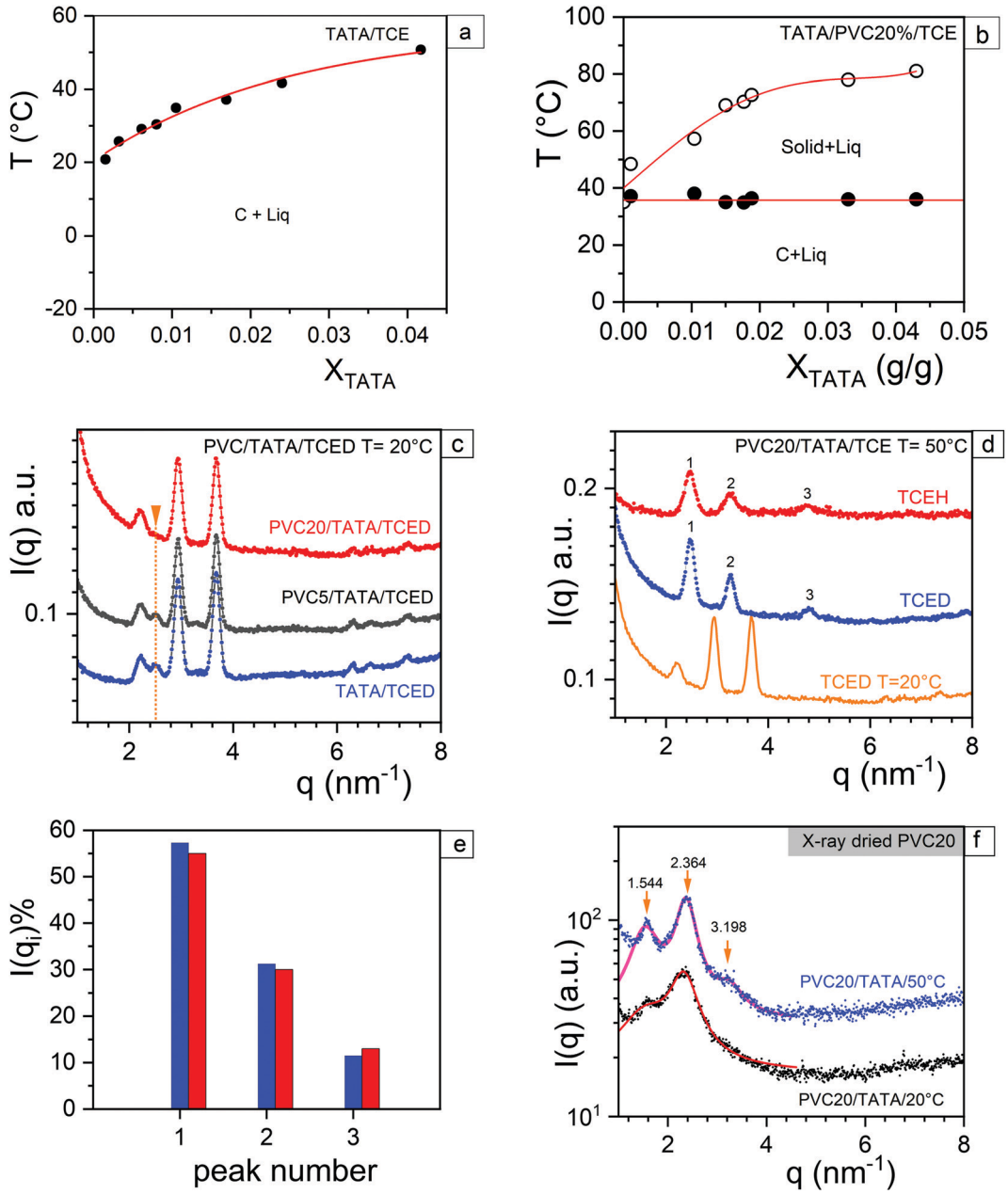

Fig. 3 (a) T–C TATA/TCE phase diagram[12] (b) PVC20/TATA/TCE phase diagram)[12] C means compound, Liq means liquid for details see ref. 13; (c): neutron diffraction pattern for TATA/TCED in different systems at T = 20 °C as indicated (C_{TATA} = 0.07 g cm^{-3}); (d) neutron diffraction pattern for PVC20/TATA/TCE at T = 50 °C, the orange line stand for the same system at 20 °C; (e) relative ratio for the first three peaks of PVC20/TATA/TCED and PVC20/TATA/TCED for T = 50 °C, blue = TCED, red = TCEH; (f) X-ray diffraction pattern for dried PVC20/TATA/TCE systems (ref. 13) processed as described in the text.

differ by nearly 40 °C,[12,13] and from their molecular structure as seen here. This situation is reminiscent of the case of crystallizable polymers,[16,26–30] where the gelation behaviour is not related to the solvent quality but to a subtle fit between the cavities created by the helical structure and the solvent shape instead. The case of polyethylene oxide (PEO) is a paradigm for illustrating this statement as the molecular compound forms depends upon the solvent isomer.[29,30] PEO compounds form with *para*-dichlorobenzene but not with *meta*- nor *ortho*-dichlorobenzene. Investigations into the effect of isomers may also provide useful information on the TATA gelation behaviour.

(2) Ternary systems PVC/TATA/solvent

In recent papers we have investigated the formation of gels prepared from PVC and self-assembling systems,[12,13,31] as well as their physical properties. Special focus has been set about on hybrid PVC/TATA/TCE gels as TATA molecules display ohmic conducting properties in this solvent.[5,6]

As far as thermodynamic properties are concerned two cases have been observed: low PVC compositions (up to 10%), and higher PVC compositions (20% and 30%).[12] For low PVC compositions the temperature-concentration phase diagram exhibits only a monotonously-increasing liquidus (melting) (Fig. 3a). For higher PVC compositions, a non-variant transformation is seen at T = 37 °C, and the terminal melting temperatures are significantly higher (Fig. 3b).

Typical results are reported in Fig. 3c for the samples in TCED for gels prepared at T = 20 °C. For the PVC5/TATA/TCED, the diffraction pattern is quite the same as that for the binary system TATA/TCED. Therefore, the unit cell portrayed in Fig. 2f still pertains to this system.

Conversely, for the PVC20/TATA/TCED gel, the small peak at q = 2.508 nm^{-1} has vanished (Fig. 2c). It is suspected that this due to a change of stoichiometry of the TATA/TCE molecular compound.

Samples investigated at T = 50 °C reveal another structure (Fig. 3d), something expected in view of the T–C phase diagram. Here, comparison of the relative intensities between TCEH and TCED reveals no significant difference (Fig. 3e). As expounded in relation 2, this indicates that the system now consists of solid phase. The thermodynamic transition occurring at T = 37 °C therefore corresponds to a total de-solvation of the compound. Although of a limited number, the peaks of this solid phase possess values quite close to those observed for structure **I** (see Table S4, ESI†). This points to a 2D orthorhombic unit cell similar to structure **I**.

Several comments can be expressed by comparison with X-ray diffraction curves previously[13] obtained on dried samples (Fig. 3f) with respect to those obtained on the wet state reported herein. Note that in Fig. 3f the sample labelled 50 °C had been heated at 50 °C in the wet state, and then was dried at this temperature so that it had undergone the non-variant transition at T = 37 °C prior to drying.

The peaks are much broader in the dried sample (FWHM ≈ 0.4 to 0.77) as compared to those measured for the present wet systems,[13] which implies a crystalline organization extending on a shorter scale. For T = 20 °C only the peak at $q \approx 2.364$ nm^{-1} is seen in neutron diffraction for the system in TCEH while another peak occurs at $q \approx 1.544$ nm^{-1} in the X-ray diffraction pattern of the dried system (Fig. 3f). For T = 50 °C, one retrieves only the peaks at $q \approx 2.364$ nm^{-1} and $q \approx 3.196$ nm^{-1} seen in the neutron diffraction curves, but not that at $q \approx 1.544$ nm^{-1}. Unsurprisingly, the drying process alters considerably the original TATA molecular structure, particularly the occurrence of a peak at $q \approx 1.544$ nm^{-1} (d = 4.07 nm) absent in the nascent state. It is worth emphasizing that the structure in the wet gel is closer to structure I observed in the solid state, while the drying process modifies markedly the nascent molecular structure.

The impact of the presence of PVC on the molecular structure of the TATA fibrils may have a bearing on recent findings on the elastic modulus of the ternary gels. As a matter of fact, the modulus of the hybrid gels largely exceeds the Voigt' upper limit,[12] an outcome hardly accountable without considering a deep modification of the intrinsic modulus of each or of one component. A de-solvation of the PVC fibrils has been envisaged which may be related to the existence of the TATA/bromobenzene molecular compound.

Concluding remarks

The neutron diffraction results presented in this paper provide a direct demonstration of the occurrence of molecular compounds in triarylamine tris-amide organogels. This study represents a rare case where the crystalline structure of organogels is investigated in their wet state. As expected, the TATA helices packing depends upon the solvent type. In particular, the molecular compound structure in TCE differs from that in benzene derivatives. This raises the question as to whether the specific packing of TATA helices in TCE modulate their conductivity properties.

Also, the present findings emphasize again that organogelation is a complex phenomenon that cannot be simply predicted by only contemplating the Hansen parameter. The propensity of forming molecular compounds between the solvent and the organogelator may play a decisive role in the final thermodynamic (phase diagram) properties of the gel and its molecular structure. This may depend on other parameters such as the solvent shape as is known in the case of polymers.[15,29,30]

Finally, the neutron diffraction technique could be extended to other systems, such as OPVOH/benzyl alcohol, where the formation of molecular compound is suspected[32] in view of the deep alteration of the gel morphology upon drying. Provided that the deuterated counterpart of the solvent is available this technique offers an unambiguous answer, especially for systems with a low number of diffraction peaks.

Conflicts of interest

The authors declare no conflict of interest.

Acknowledgements

The authors acknowledge access to the D16 diffractometer at the ILL through DOI: 10.5291/ILL-DATA.9-11-2058.

References

1 H. Kawai, The piezoelectricity of poly(vinylidene fluoride), *Jpn. J. Appl. Phys.*, 1969, **8**, 1975.
2 R. Hasegawa, Y. Takahashi, Y. Chatani and H. Tadokoro, Crystal structures of three crystalline forms of poly(vinylidene fluoride), *Polym. J.*, 1972, **3**, 600.
3 G. Guerra, C. Manfredi, P. Musto and S. Tavone, Guest conformation and diffusion into amorphous and emptied clathrate phases of syndiotactic polystyrene, *Macromolecules*, 1998, **31**, 1329.
4 C. Daniel, D. Alfano, V. Venditto, S. Cardea, E. Reverchon, D. Larobina, G. Mensitieri and G. Guerra, Aerogels with a microporous crystalline host phase, *Adv. Mater.*, 2005, **17**, 1515.
5 E. Moulin, J. J. Armao IV and N. Giuseppone, Triaryl amine-based supramolecular polymers: Structure, dynamics, and functions, *Acc. Chem. Res.*, 2019, **52**, 975.
6 J. J. Armao IV, M. Maaloum, T. Ellis, G. Fuks, M. Rawiso, E. Moulin and N. Giuseppone, Healable supramolecular polymers as organic metals, *J. Am. Chem. Soc.*, 2014, **136**, 11382.
7 Molecular compound is a generic term for designating inclusion compounds, clathrates, intercalates, crystallosolvates, host–guest compounds, complexes,…. See for example: A. Reisman, *Phase Equilibria: Basic Principles, Applications, Experimental Techniques*, Elsevier, 1970; and more recently J. M. Guenet, *Polymer-solvent molecular compounds*, Elsevier, London, 2008.
8 S. J. George, Z. Tomovic, A.P. H. J. Schenning and E. W. Meijer, Insight into the chiral induction in supramolecular stacks through preferential chiral solvation, *Chem. Commun.*, 2011, **47**, 3451.
9 K. K. Kartha, S. S. Babu, S. Srinivasan and A. Ajayaghosh, Attogram sensing of trinitrotoluene with a self-assembled molecular gelator, *J. Am. Chem. Soc.*, 2012, **134**, 4834.
10 K. K. Kartha, A. Sandeep, V. K. Praveen and A. Ajayaghosh, Detection of nitroaromatic explosives with fluorescent molecular assemblies and π-gels, *Chem. Rec.*, 2015, **15**, 252.
11 J. M. Guenet, *Organogels: Thermodynamics, structure, solvent role and properties*, Springer International Publishing, NY, 2016.
12 B. Kiflemariam, D. Collin, O. Gavat, A. Carvalho, E. Moulin, N. Giuseppone and J. M. Guenet, Hybrid materials from triaryl amine organogelators and poly[vinyl chloride] networks, *Polymer*, 2020, **207**, 122814.
13 P. Talebpour, B. Heinrich, O. Gavat, A. Carvalho, E. Moulin, N. Giuseppone and J. M. Guenet, Modulation of the molecular structure of tri-aryl amine fibrils in hybrid poly[vinyl chloride] gel/organogel systems, *Macromolecules*, 2021, **54**, 8104.
14 R. E. Rundle, C. G. Schull and E. O. Wollan, The crystal structure of thorium and zirconium dihydrides by X-ray and neutron diffraction, *Acta Crystallogr.*, 1952, **5**, 22.
15 J. J. Point, P. Damman and J. M. Guenet, Neutron diffraction study of poly(ethylene oxide) p dihalogenobenzene crystalline complexes, *Polym. Commun.*, 1991, **32**, 477.
16 C. Daniel, A. Menelle, A. Brulet and J. M. Guenet, Thermoreversible gelation of syndiotactic polystyrene in toluene and chloroform, *Polymer*, 1997, **38**, 4193.
17 F. Kaneko, N. Seto, S. Sato, A. Radulescu, M. M. Schiavone, J. Allgaier and K. Ute, Development of a simultaneous SANS/FTIR measuring system, *Chem. Lett.*, 2015, **44**, 497.
18 G. E. Bacon, Coherent neutron-scattering amplitudes, *Acta Crystallogr., Sect. A: Cryst. Phys., Diffr., Theor. Gen. Crystallogr.*, 1972, **28**, 357.
19 V. Cristiglio, B. Giroud, L. Didier and B. Demé, D16 is back to business: More neutrons, more space, more fun, *Neutron News*, 2015, **26**, 23.
20 P. Mittelbach and G. Porod, Zur Röntgenkleinwinkelstreuung verdünnter kolloiden Systeme, *Acta Phys. Austriaca*, 1961, **14**, 185.
21 O. A. Pringle and P. W. Schmidt, Small-angle X-ray scattering from helical macromolecules, *J. Appl. Crystallogr.*, 1971, **4**, 290.
22 M. Raynal and L. Bouteiller, Organogel formation rationalized by Hansen solubility parameters, *Chem. Commun.*, 2011, **47**, 8271.
23 N. Yan, Z. Xu, K. K. Diehn, S. R. Raghavan, Y. Fang and R. G. Weiss, How do liquid mixtures solubilize insoluble gelators? Self-assembly properties of pyrenyl-glucono gelators in tetrahydrofuran–water mixtures, *JACS*, 2013, **135**, 8989.
24 J. Bonnet, G. Suissa, M. Raynal and L. Bouteiller, Organogel formation rationalized by Hansen solubility parameters: Dos and don'ts, *Soft Matter*, 2014, **10**, 3154.
25 J. E. Mark, *Physical Properties of Polymer Handbook*, Springer, NY, 2nd edn, 2007, p. 1076.
26 A. Immirzi, F. de Candia, P. Ianelli, A. Zambelli and V. Vittoria, Solvent-induced polymorphism in syndiotactic polystyrene, *Makromol. Chem. Rapid Commun*, 1988, **9**, 761.
27 Y. Chatani, Y. Shimane, T. Inagaki, T. Ijitsu, T. Yukinari and H. Shikuma, Structural study on syndiotactic polystyrene: 2. Crystal structure of molecular compound with toluene, *Polymer*, 1993, **34**, 1620.
28 Y. Chatani and M. Nakamura, Coiled-coil molecular model for isotactic polystyrene gels, *Polymer*, 1993, **34**, 1644.
29 J. J. Point and C. Coutelier, Linear high polymers as host in intercalates. Introduction and example, *J. Polym. Sci. Polym. Phys*, 1985, **23**, 231.
30 J. J. Point, C. Coutelier and D. Villers, Intercalates with linear polymer host. Part 4. Structure of p-C6H4XY-polyoxyethylene) intercalates from unit-cell determination and energy minimization, *J. Phys. Chem.*, 1986, **90**, 3277.
31 Z. Zoukal, S. Elhasri, A. Carvalho, M. Schmutz, D. Collin, P. K. Vakayil, A. Ajayaghosh and J. M. Guenet, Hybrid materials from poly[vinyl chloride] and organogels, *ACS Appl. Polym. Mater.*, 2019, **1**, 1203.
32 D. Dasgupta, S. Srinivasan, C. Rochas, A. Ajayaghosh and J. M. Guenet, Solvent-mediated fiber growth in organogels, *Soft Matter*, 2011, **7**, 9311.